Chapter 1

New Insights and Horizons from the Linear Response Function in Conceptual DFT

Paul Geerlings, Stijn Fias, Thijs Stuyver, Paul Ayers, Robert Balawender and Frank De Proft

Additional information is available at the end of the chapter

http://dx.doi.org/10.5772/intechopen.80280

Abstract

An overview is given of our recent work on the linear response function (LRF) $\chi(\mathbf{r}, \mathbf{r}')$ and its congener, the softness kernel $s(\mathbf{r}, \mathbf{r}')$, the second functional derivatives of the energy E and the grand potential Ω with respect to the external potential at constant N and μ, respectively. In a first section on new insights into the LRF in the context of conceptual DFT, the mathematical and physical properties of these kernels are scrutinized through the concavity of the $E = E[N, v]$ and $\Omega = \Omega[\mu, v]$ functionals in $v(\mathbf{r})$ resulting, for example, in the negative semidefiniteness of χ. As an example of the analogy between the CDFT functionals and thermodynamic state functions, the analogy between the stability conditions of the macroscopic Gibbs free energy function and the concavity conditions for Ω is established, yielding a relationship between the global and local softness and the softness kernel. The role of LRF and especially the softness kernel in Kohn's nearsightedness of electronic matter (NEM) principle is highlighted. The first numerical results on the softness kernel for molecules are reported and scrutinized for their nearsightedness, reconciling the physicists' NEM view and the chemists' transferability paradigm. The extension of LRF in the context of spin polarized conceptual DFT is presented. Finally, two sections are devoted to 'new horizons' for the LRF. The role of LRF in (evaluating) alchemical derivatives is stressed, the latter playing a promising role in exploring the chemical compound space. Examples for the transmutation of N_2 and the CC → BN substitution pattern in 2D and 3D carbocyclic systems illustrate the computational efficiency of the use of alchemical derivatives in exploring nearest neighbours in the chemical compound space. As a second perspective, the role of LRF in evaluating and interpreting molecular conductivity is described. Returning to its forerunner, Coulson's atom-atom polarizability, it is shown how in conjugated π systems (and within certain approximations) a remarkable integral-integrand relationship between the atom-atom polarizability and the transmission probability between the atoms/contacts exists, leading to similar trends in both properties. A simple selection rule for transmission probability in alternating hydrocarbons is derived based on the sign of the atom-atom polarizability.

Keywords: conceptual DFT, linear response function, nearsightedness of electronic matter, alchemical derivatives, molecular conductivity

1. Introduction

A continuous challenge for theoretical and quantum chemists is to see if 'classical' chemical concepts describing bonding, structure and reactivity—the common language of all chemists—can still be retrieved from the nowadays extensive and complex computational results obtained at different levels of complexity with wave function or density functional theory. Conceptual density functional theory (CDFT) [1–6] has played an important role in this endeavour in the past decades. CDFT is a branch of DFT [7, 8] aiming to give precision to often well-known but sometimes vaguely defined chemical concepts (e.g. electronegativity, hardness and softness), affording their numerical evaluation, and to use them either as such or in the context of principles such as Sanderson's electronegativity equalization principle [9] or Pearson's hard and soft acids and bases principle [10]. 'Chemical' DFT or even 'chemical reactivity' DFT would have been a better name for the obvious reason that concepts are essential for all branches of DFT (especially the fundamentals) and that chemical reactivity is one of the main issues addressed in conceptual DFT.

When looking at the basics of CDFT, the energy functional, $E = E[N, v]$, stands out [8]. Why? It is the key ingredient to get (qualitative and quantitative) insight into the eagerness of an atom, or a molecule, to adapt itself to changes in the number of electrons, N, and/or the external potential, $v(\mathbf{r})$, that is, the potential felt by the electrons due to the nuclei. These changes are essential in describing (the onset of) a chemical reaction, hence chemical reactivity. The readiness of a system to adapt itself to these new conditions is quantified through *response functions*, $\delta^m(\partial^n E/\partial N^n)/\delta v(\mathbf{r}_1)\ldots\delta v(\mathbf{r}_m)$, which are the cornerstones of CDFT. Literature on these response functions is abundant, especially on the first-order responses (electronic chemical potential μ [11] $(n = 1, m = 0)$ and the electron density $\rho(\mathbf{r})$ $(n = 0, m = 1)$, the cornerstone of DFT itself) and two of the second-order responses (chemical hardness η $(n = 2, m = 0)$ and its inverse, the chemical softness S [12], and the electronic Fukui function $f(\mathbf{r})(n = 1, m = 1)$ [13]). The most prominent of the third-order response functions [14] is the dual descriptor $f^{(2)}(\mathbf{r})$ [15], the N-derivative of the Fukui function $(n = 1, m = 1)$. Remarkably, response functions diagonal in $v(\mathbf{r})$ $(n = 0, m = 2 - 3)$ were nearly absent in the CDFT literature until about 10 years ago (see [16] for an overview of this early work). The reasons are obvious; here we concentrate on its simplest member $(n = 0, m = 2)$, the linear response function (LRF).

$$\chi(\mathbf{r}, \mathbf{r}') = \left(\delta^2 E/\delta v(\mathbf{r})\delta v(\mathbf{r}')\right)_N \tag{1}$$

The calculation of this kernel turns out to be far from trivial, as is the representation of this quantity, a function of six Cartesian coordinates, and by extension its link to 'chemical' concepts.

Note that in the context of time-dependent DFT [17–19], the LRF has made its appearance many years ago as it was realized that the poles of its frequency-dependent form are nothing other than the electronic excitation energies. Thanks to Casida's elegant matrix formalism [20], electronic transition frequencies, intensities and assignments are nowadays routinely performed, implemented as they are in standard quantum chemistry packages. However, this evolution was not accompanied by a parallel endeavour on the evaluation, representation and chemical interpretation of the frequency-independent or static LRF.

In the past decade, the ALGC group, in collaboration with colleagues from different countries (Canada (Ayers), US (Yang), Spain (Sola), Poland (Balawender), etc.), set out a program aiming at the systematic evaluation, representation and interpretation of the LRF with the following results obtained until 2013, summarized in a review paper in Chemical Society Reviews [16] (no explicit reference to each of the individual constituting studies will be given).

1. The LRF can now be routinely calculated at several levels of approximation for which the coupled perturbed Kohn-Sham perturbational approach turns out to be the most attractive approach, also permitting different levels of sophistication depending on the treatment of the exchange correlation potential (v_{xc}) term in the perturbation equations. In its simplest form (neglecting the influence of the external potential variation on the Coulomb and exchange-correlation terms in the perturbational equations), the independent particle expression, already presented by Ayers and Parr [8, 21], is retrieved.

2. The representation can be done via contour diagrams (fixing, e.g. r′) as demonstrated for atoms and molecules, or in the case of molecules, after condensation, via a simple atom-atom matrix, reminiscent of reporting the results of a population analysis.

3. An abundance of chemical information was shown to be present in the LRF ranging from the shell structure of atoms, to inductive and mesomeric effects, electron (de)localization and (anti)aromaticity in molecules.

In the present chapter, a synopsis is given of the progress made since then by the ALGC group in collaboration with other groups as witnessed by two of the authors (P.A and R. B.), both on fundamental and applied aspects, that is, on *new insights* into the properties of the LRF and on *new areas* where the LRF is at stake. In Section 2 the mathematical/physical properties of the LRF are revised together with those of its congener, the softness kernel $s(\mathbf{r}, \mathbf{r}')$, the latter playing a fundamental role in scrutinizing Kohn's nearsightedness of electronic matter (NEM) principle. The extension of LRF in the context of spin polarized DFT is also addressed. In Section 3, we highlight the importance of the LRF in the emerging field of alchemical derivatives when exploring the chemical compound space. We illustrate the potential of alchemical derivatives in exploring the CC → BN isoelectronic substitution in 2D and 3D unsaturated carbocyclic molecules: benzene and the C_{60} fullerenes. Finally, in Section 4 we show how the LRF (in fact its forerunner, Coulson's atom-atom polarizability) can be used to predict/interpret the conductivity behaviour of unsaturated hydrocarbons, thus entering the vibrant field of molecular electronics.

2. Theoretical developments

2.1. On the negative and positive semidefiniteness of the LRF and the softness kernel and thermodynamic analogies

The properties of the LRF $\chi(\mathbf{r}, \mathbf{r}')$ are intimately related to the concavity/convexity properties of $E[N, v]$ that we addressed in recent years [22, 23]. Where $E[N, v]$ is convex with respect to (w.r.t.) N [24], it is well established that $E[N, v]$ is concave w.r.t. $v(\mathbf{r})$ following the Jensen's inequality.

$$E[N, \lambda v_1 + (1-\lambda)v_2] \geq \lambda E[N, v_1] + (1-\lambda)E[N, v_2] \qquad \wedge \quad \lambda \in [0, 1] \tag{2}$$

(see for example Lieb [25], Eschrig [26], and Helgaker et al. [27]). In **Figure 1** (after Helgaker [28]) we illustrate the physical interpretation of this concavity property. For a given potential v_1, the associated ground state energy is given by the expectation value $\langle \psi_1 | H[v_1] | \psi_1 \rangle$, with ground state wave function ψ_1, the red point in the figure. Changing v_1 to v_2, with constant ψ, induces changes in energy linear in $\delta v(\mathbf{r})$ as a consequence of the term $\int \rho(\mathbf{r}) v(\mathbf{r}) d\mathbf{r}$ in the DFT energy expression. Relaxing the wave function yields an energy lowering (blue arrow) until the energy obtained by applying the variational principle with $v = v_2$ is reached (with associated wave function ψ_2). Consequently, the true energy (black line) will always be found below the tangent line ensuring concavity.

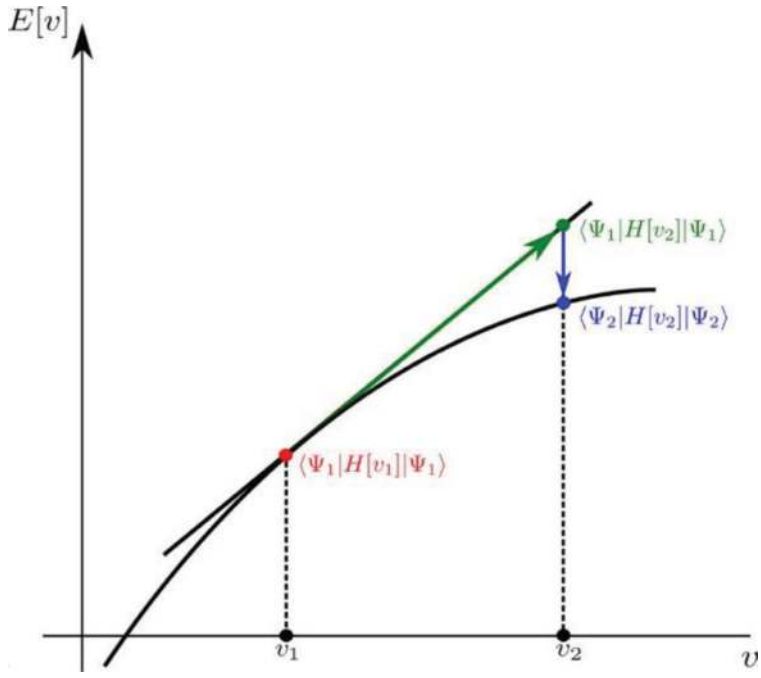

Figure 1. Illustration of the concavity of the $E = E[v]$ functional (after Helgaker [28]) (Reprinted by permission from Springer Nature, Copyright 2016 [22]).

A direct consequence is that the LRF is negative semidefinite.

$$\iint \chi(\mathbf{r},\mathbf{r}')\theta(\mathbf{r})\theta(\mathbf{r}')d\mathbf{r}d\mathbf{r}' \leq 0 \tag{3}$$

where $\theta(\mathbf{r})$ is any continuous function [23]. This inequality shows up when considering the second-order variation of the energy

$$\delta E^{(2)} = \tfrac{1}{2}\iint \left(\delta^2 E/\delta v(\mathbf{r})\delta v(\mathbf{r}')\right)_N \delta v(\mathbf{r})\delta v(\mathbf{r}')d\mathbf{r}d\mathbf{r}' \tag{4}$$

When adopting the $\delta v(\mathbf{r}) = V_0\delta(\mathbf{r}-\mathbf{r}'')$ choice for $\delta v(\mathbf{r})$, where V_0 is a constant one gets

$$\delta E^{(2)} = \tfrac{1}{2}V_0^2\chi(\mathbf{r}'',\mathbf{r}'') \leq 0 \tag{5}$$

showing that the diagonal elements of the linear response function $\chi(\mathbf{r},\mathbf{r}')$ should be negative or zero. This result links the concavity of the $E[N,v]$ functional to the diagonal elements of the linear response function defined on $R^3 \times R^3$. This negativity was retrieved in all our numerical results (non-integrated and condensed) (see for example [29, 30]). Its physical interpretation is straightforward through the definition of $\chi(\mathbf{r},\mathbf{r}')$ as $(\delta\rho(\mathbf{r})/\delta v(\mathbf{r}'))_N$: if the potential at a given point $\mathbf{r}$ is increased (made less negative), this electron-unfavourable situation will lead to electron depletion at that point, yielding a negative $\chi(\mathbf{r},\mathbf{r})$.

In Section 4, we will point out that Coulson's atom-atom polarizability π_{AB} [31] can be considered as a Hückel-theory forerunner of the LRF and exploit its properties in discussing molecular conductivity. Defined as

$$\pi_{AB} = \partial q_A/\partial\alpha_B = \partial^2 E/\partial\alpha_A\partial\alpha_B = \pi_{BA} \tag{6}$$

the analogy emerges as q_A is the π-electron charge on atom A, whereas (the change in) the Coulomb integral α_B is equivalent to a change in the external potential. The case $A = B$ was explored by Coulson using his complex integral formalism for Hückel's π energy and its derivatives, proving that π_{AA} can be written as

$$\pi_{AA} = (1/\pi)\int_{-\infty}^{+\infty} (\Delta_{AA}(iy)/\Delta(iy))^2 dy \tag{7}$$

Here, Δ represents the Hückel secular determinant (or characteristic function) and Δ_{AA} is its counterpart with row A and column A deleted. It turns out that $\Delta_{AA}(iy)/\Delta(iy)$ is imaginary and therefore π_{AA} is negative (see also Section 4).

When introducing the $E = E[N,v]$ functional, it was stressed that in the LRF the second functional derivative is taken at constant N. In the remaining part of this chapter, it turns out that no less important role in CDFT is played by the softness kernel, which is the second functional derivative with respect to $v(\mathbf{r})$ of the $\Omega = \Omega[\mu,v]$ functional (the grand potential)

at constant μ. Here, we switch from the canonical ensemble to the grand canonical ensemble [32] connecting two ways of specifying the same physics via functionals of each time two variables differing in one pair that is connected through a Legendre transformation (see for example [33]).

$$\Omega\left[\mu, v\right] = E\left[\tilde{N}\left[\mu, v\right], v\right] - \mu\tilde{N}\left[\mu, v\right] \tag{8}$$

where μ and N are conjugate variables which are related by identities $\tilde{N}\left[\mu, v\right] = N$ and $\tilde{\mu}[N, v] = \mu$. Its apparent analogy with classical thermodynamics will be addressed later.

In [23], we pointed out that $\Omega\left[\mu, v\right]$ just as $E[N, v]$ is concave w.r.t. $v(\mathbf{r})$, implying that its second functional derivative at constant μ, the softness kernel (note the negative sign in the definition) [34].

$$s(\mathbf{r}, \mathbf{r}') = -\left(\delta^2\Omega/\delta v(\mathbf{r})\delta v(\mathbf{r}')\right)_{\mu} \tag{9}$$

is positive semidefinite. This property fits the well-known Berkowitz-Parr relationship [33] linking $\chi(\mathbf{r}, \mathbf{r}')$ and $s(\mathbf{r}, \mathbf{r}')$ (vide infra).

$$s(\mathbf{r}, \mathbf{r}') = -\chi(\mathbf{r}, \mathbf{r}') + f(\mathbf{r})f(\mathbf{r}')/\eta \tag{10}$$

where $f(\mathbf{r})$ is the Fukui function and η is the hardness. Indeed,

$$\begin{aligned} \iint s(\mathbf{r}, \mathbf{r}')\theta(\mathbf{r})\theta(\mathbf{r}')d\mathbf{r}d\mathbf{r}' &= \iint (-\chi(\mathbf{r}, \mathbf{r}') + f(\mathbf{r})f(\mathbf{r}')/\eta)\theta(\mathbf{r})\theta(\mathbf{r}')d\mathbf{r}d\mathbf{r}' \\ &= -\iint \chi(\mathbf{r}, \mathbf{r}')\theta(\mathbf{r})\theta(\mathbf{r}')d\mathbf{r}d\mathbf{r}' + 1/\eta \int (f(\mathbf{r})\theta(\mathbf{r}))^2 d\mathbf{r} \geq 0 \end{aligned} \tag{11}$$

since the hardness is nonnegative and $\chi(\mathbf{r}, \mathbf{r}')$ was shown to be negative semidefinite.

The properties of $\chi(\mathbf{r}, \mathbf{r}')$ and $s(\mathbf{r}, \mathbf{r}')$ incited us to reconsider the analogy between the DFT functionals E and Ω [32] on the one hand and the macroscopic thermodynamic state functions $U = U[S, V]$, $F = F[T, V]$, $H = H[S, P]$ and $G = G[T, P]$ on the other hand (internal energy, Helmholtz free energy, enthalpy and Gibbs free energy written as functions of volume (V), temperature (T), pressure (P) and entropy (S)). Parr and Nalewajski extended the notion of intensive and extensive variables (T, P) and (S, V), respectively, in thermodynamics to the variables in DFT functionals by classifying external variables as properties additive with respect to any partitioning of the electron density $\rho(\mathbf{r}) = \rho_A(\mathbf{r}) + \rho_B(\mathbf{r})$ [32]. In this way, $\rho(\mathbf{r})$ and N are clearly extensive, and μ and $v(\mathbf{r})$ are intensive. The analogy between $G[T, P]$ and $\Omega\left[\mu, v\right]$ can now be stressed: both the state function G and the DFT functional Ω contain two intensive variables. This situation leads to a remarkable property when formulating a DFT analogue of the stability analysis in macroscopic thermodynamics [33, 35, 36]. Concavity for $G[T, P]$ in all directions then implies that

$$d^2G = G_{TT}(\Delta T)^2 + 2G_{TP}\Delta T\Delta P + G_{PP}(\Delta P)^2 \leq 0, \tag{12}$$

where G_{TT}, G_{TP} and G_{PP} are the second derivatives of Gibbs free energy, $\left(G_{XY} = \partial^2 G/\partial X \partial Y\right)$. This stability condition implies the negative semidefiniteness of the Hessian matrix. It yields

$$G_{PP} = (\partial V/\partial P)_T = -\kappa_T V \leq 0 \tag{13}$$

$$G_{TT} = -(\partial S/\partial T)_P = -C_P/T \leq 0 \tag{14}$$

that is, the isothermal compressibility κ_T and the heat capacity at constant pressure C_P should be positive, and the condition that

$$\left(G_{TT}G_{PP} - G_{PT}^2\right) = \left(\kappa_T V C_P/T - \alpha^2 V^2\right) \geq 0 \Leftrightarrow \kappa_T C_P/T \geq \alpha^2 V \tag{15}$$

where $\alpha = (\partial V/\partial T)_P/V$ is the coefficient of thermal expansion. Another classical example of such stability analysis is the entropy written as $S[U, V]$ (at constant number of particles) where both variables are now extensive [33].

Let us now consider the analogy with $\Omega\left[\mu, v\right]$. It is well known that

$$\left(\partial^2\Omega/\partial\mu^2\right)_v = -S\left[\mu, v\right], \tag{16}$$

where S is the global softness [3]. As the r.h.s. of (16) is negative, concavity for $\Omega\left[\mu, v\right]$ in μ shows up. As discussed above, Ω is also concave in $v(\mathbf{r})$, leading to the positive semidefiniteness of $s(\mathbf{r}, \mathbf{r}')$ (these expressions being the counterparts of (13) and (14)). The condition for concavity in all directions leads after some algebra (see [23]) to the condition

$$\left(\left(\partial^2\Omega/\partial\mu^2\right)_v \Delta\mu + \int \left(\partial(\delta\Omega/\delta v(\mathbf{r}))_\mu/\partial\mu\right)_v \Delta v(\mathbf{r}) d\mathbf{r}\right)^2 + \iint \left(\left(\partial^2\Omega/\partial\mu^2\right)_v \left(\delta^2\Omega/\delta v(\mathbf{r})\delta v(\mathbf{r}')\right)_\mu \right.$$
$$\left. - \left(\partial(\delta\Omega/\delta v(\mathbf{r}))_\mu/\partial\mu\right)_v \left(\partial(\delta\Omega/\delta v(\mathbf{r}'))_\mu/\partial\mu\right)_v\right) \Delta v(\mathbf{r}) d\mathbf{r} \Delta v(\mathbf{r}') d\mathbf{r}' \geq 0 \tag{17}$$

and finally to

$$\iint \left(s(\mathbf{r}, \mathbf{r}')S - s(\mathbf{r})s(\mathbf{r}')\right) \Delta v(\mathbf{r}) d\mathbf{r} \Delta v(\mathbf{r}') d\mathbf{r}' \geq 0, \tag{18}$$

the analogue of (15) where the local softness

$$s(\mathbf{r}) = \left(\partial(\delta\Omega/\delta v(\mathbf{r}))_\mu/\partial\mu\right)_v = \left(\partial\rho(\mathbf{r})/\partial\mu\right)_v \tag{19}$$

has been introduced [37]. Taking again for $\Delta v(\mathbf{r})$ and $\Delta v(\mathbf{r}')$ Dirac delta functions $\delta(\mathbf{r} - \mathbf{r}'')$ and $\delta(\mathbf{r}' - \mathbf{r}'')$, one obtains the condition

$$s(\mathbf{r}, \mathbf{r})S \geq \left(s(\mathbf{r})\right)^2 \geq 0. \tag{20}$$

This inequality shows that the diagonal elements $s(\mathbf{r}, \mathbf{r})$ should be positive, as could be inferred from the concavity of $\Omega\left[\mu, v\right]$ but, more importantly, they impose a restriction on the relative

values of the three softness descriptors $s(\mathbf{r},\mathbf{r}')$,$S$ and $s(\mathbf{r})$ in analogy to the thermodynamic relationship between κ_T, C_P and α at given T and P ($V = V[T,P]$). This result is compatible with the aforementioned Berkowitz-Parr relationship. Indeed, starting from their expression for $\mathbf{r}' = \mathbf{r}$ (see (10), the relations $s(\mathbf{r}) = f(\mathbf{r})/\eta$)

$$s(\mathbf{r},\mathbf{r}) = -\chi(\mathbf{r},\mathbf{r}) + s(\mathbf{r})s(\mathbf{r})/S \tag{21}$$

and knowing that $\chi(\mathbf{r},\mathbf{r}) \leq 0$ (vide supra) one obtains

$$s(\mathbf{r},\mathbf{r}) - s(\mathbf{r})s(\mathbf{r})/S \geq 0, \tag{22}$$

retrieving our conclusions above.

2.2. Kohn's nearsightedness of electronic matter revisited

We now report on our recent explorations [38] on Kohn's NEM principle. Kohn introduced the NEM concept in 1996 [39] and elaborated on it in 2005 with Prodan et al. [40]. In his own words, it can be viewed as 'underlying such important ideas as Pauling's chemical bond, transferability, and Yang's computational principle of divide and conquer' [40]. Certainly in view of the two former issues, this principle, formulated by a physicist, touches the very heart of chemistry and so, in our opinion, it was tempting to look at it with a chemist's eye. Why however is this issue addressed in this chapter; in other words, what is the link between the LRF and nearsightedness?

The quintessence of the NEM principle is as follows (**Figure 2**): consider a (many) electron system characterized by an electron density function $\rho(\mathbf{r})$ with a given electronic chemical potential μ. Now, concentrate on a point $\mathbf{r}_0$ and perturb the system in its external potential $v(\mathbf{r})$ at point $\mathbf{r}'$, outside a sphere with radius R around $\mathbf{r}_0$ at constant electronic potential μ. Then, the NEM principle states that the absolute value of the density change at $\mathbf{r}_0$, $|\Delta\rho(\mathbf{r}_0)|$, will be lower than a finite maximum value $\overline{\Delta\rho}$, which depends on $\mathbf{r}_0$ and R, whatever the magnitude of the perturbation. As stated by Kohn, anthropomorphically the particle density $\rho(\mathbf{r})$cannot 'see' any perturbation $v(\mathbf{r})$ beyond the distance $R\left[\mathbf{r}_0, \overline{\Delta\rho}\right]$ within an accuracy $\overline{\Delta\rho}$, that is, the density shows nearsightedness. Kohn offered evidence that in the case of 1D 'gapped' systems (i.e. with hardness η larger than zero) the decay of $\overline{\Delta\rho}$ as a function of R (i.e. upon increasing $|\mathbf{r} - \mathbf{r}_0|$) is exponential and that for gapless systems it follows a power law. This suggests that in the molecular world, where η is observed to be always positive, the electron density should only be sensitive to nearby changes in the external potential. In [38], we provided the first numerical confirmation of this nearsightedness principle for real, 3D, molecules.

Again, why address this issue in this LRF chapter? Going back to Kohn's formulation quintessentially a change in density at a given point $\Delta\rho(\mathbf{r}_0)$ in response to a change in external potential $\Delta v(\mathbf{r}')$ at different points is analysed. These are the typical ingredients of the LRF (change in v produces a change in ρ), and in this case the process is considered at constant electronic chemical potential μ, in order words $(\delta\rho(\mathbf{r})/\delta v(\mathbf{r}'))_\mu$ is the key quantity. This is nothing else than the softness kernel $s(\mathbf{r},\mathbf{r}')$ with a minus sign in front. Indeed,

http://dx.doi.org/10.5772/intechopen.80280

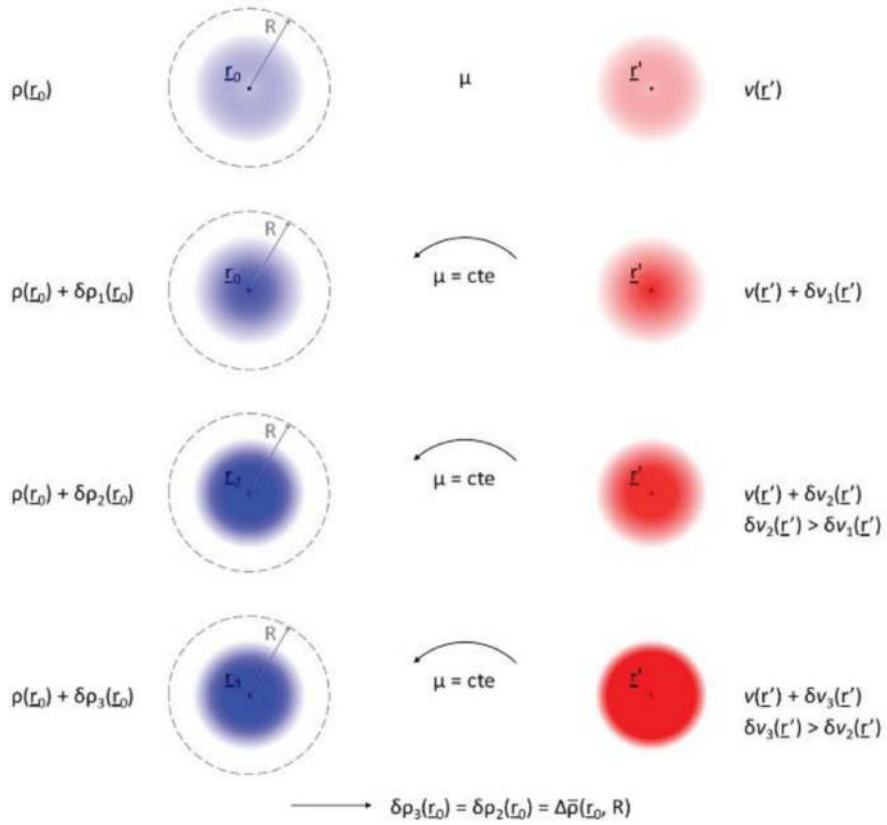

Figure 2. Pictorial representation of the nearsightedness of electronic matter principle: when $\delta v(\mathbf{r}') \geq \delta v_2(\mathbf{r}')$, with $\mathbf{r}'$ outside a sphere with radius R around r_0, $\delta\rho_0(r_0)$ no longer increases—$\delta\rho_0(\mathbf{r}_0) = \overline{\Delta\rho}(\mathbf{r}_0, R)$ no matter how large $\delta v(\mathbf{r}')$. The intensity of the red and blue regions represents the magnitude of $v(\mathbf{r}')$ and $\rho(\mathbf{r})$, respectively.

$$\left(\delta\rho(\mathbf{r})/\delta v(\mathbf{r}')\right)_{\mu} = -s(\mathbf{r},\mathbf{r}') = \left(\delta^2\Omega/\delta v(\mathbf{r})\delta v(\mathbf{r}')\right)_{\mu} \tag{23}$$

The Berkowitz-Parr relationship [34] can then be written as

$$\left(\delta\rho(\mathbf{r})/\delta v(\mathbf{r}')\right)_{N} = \left(\delta\rho(\mathbf{r})/\delta v(\mathbf{r}')\right)_{\mu} - \left(\partial\rho(\mathbf{r})/\partial\mu\right)_{v}\left(\delta\mu/\delta v(\mathbf{r}')\right)_{N} \tag{24}$$

an equation transforming conditions of constant N into constant μ, for taking the functional derivative of $\rho(\mathbf{r})$ w.r.t. $\delta v(\mathbf{r})$ in analogy with this type of equation for partial derivatives in macroscopic thermodynamics [33]. As $\left(\partial\rho(\mathbf{r})/\partial\mu\right)_{v}$ equals the local softness $s(\mathbf{r})$ and $\left(\delta\mu/\delta v(\mathbf{r}')\right)_{N}$ is an alternative way, as compared to $\left(\partial\rho(\mathbf{r})/\partial N\right)_{v}$ to write the Fukui function f(r), one retrieves from (28)

$$s(\mathbf{r},\mathbf{r}') = -\chi(\mathbf{r},\mathbf{r}') + f(\mathbf{r})f(\mathbf{r}')/\eta \tag{25}$$

which will be the key equation in this section. As analytical methods are available to evaluate $\chi(\mathbf{r},\mathbf{r}')$, $f(\mathbf{r})$ and η on equal footing [41], $s(\mathbf{r},\mathbf{r}')$ can be evaluated, and its difference with $\chi(\mathbf{r},\mathbf{r}')$ analysed, in order to scrutinize nearsightedness.

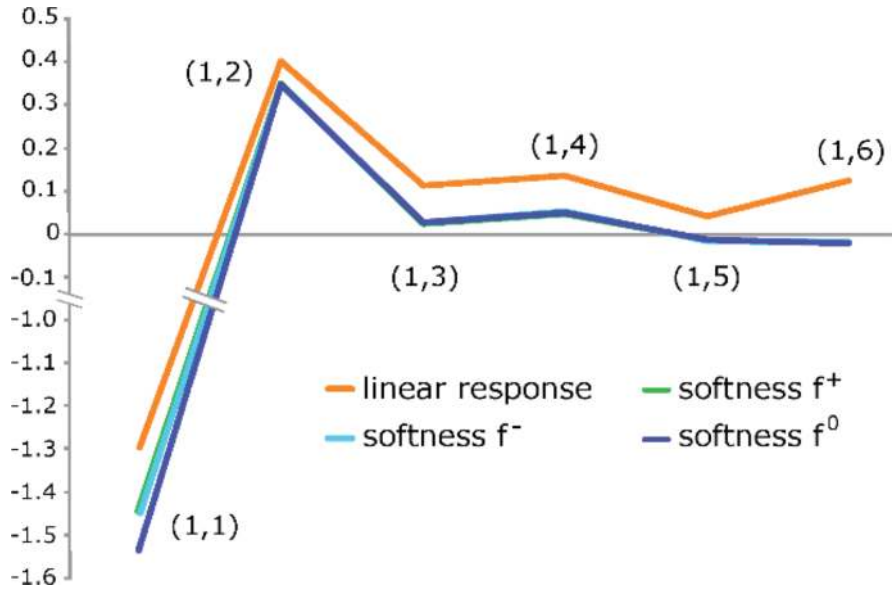

Figure 3. Atom condensed linear response function and softness kernel of 1,3,5-hexatriene. The curves of the softness kernels using f+ and f− are overlapping [38].

In **Figure 3**, we depict the atom condensed linear response function and the softness kernel, the matrices χ_{AB} and s_{AB}, of 1,3,5-hexatriene. Condensation was performed by integrating the kernels over the domains of atoms A and B, represented by V_A and V_A, that is,

$$s_{AB} = \int_{V_A}\int_{V_B} s(\mathbf{r},\mathbf{r}')d\mathbf{r}d\mathbf{r}' \tag{26}$$

From our previous work on polyenes [42], the χ_{AB} matrix elements are known to show an alternating behaviour with maxima on mesomeric active atoms (C_2,C_4 and C_6) and minima for mesomeric passive atoms (C_3 and C_5), with the change in $v(\mathbf{r})$ taking place at C_1.The picture illustrates that the softness kernel is more nearsighted than the LRF (all its values are lower) and that $s_{1,5}$ and $s_{1,6}$ are very close to zero; the effect of the perturbation has died off completely, confirming the nearsightedness of the softness kernel. This effect can be traced back to a cancellation of the LRF, which is non-nearsighted, by the second term in Eq. (25), and accounts for the density changes induced by charge transfer from the electron reservoir to keep the chemical potential constant. Note that this condition, at first sight somewhat strange, is an often more realistic perspective when considering for example the reactivity of molecules in solution where the chemical potential is fixed by the solvent allowing (partial) charge transfer to or from the molecule while keeping its chemical potential constant [43, 44].

As a second example, we show in **Figure 4** the change in density of the 1,3,5-heptatrienyl cation when the C atom of one of the terminal CH_2 atoms was alchemically replaced by an N atom. The corresponding density difference was evaluated through the alchemical derivatives approach (Section 3) where the carbon atom of the CH_2 group was annihilated and replaced by a nitrogen atom at constant geometry and constant number of electrons. It is clear that the

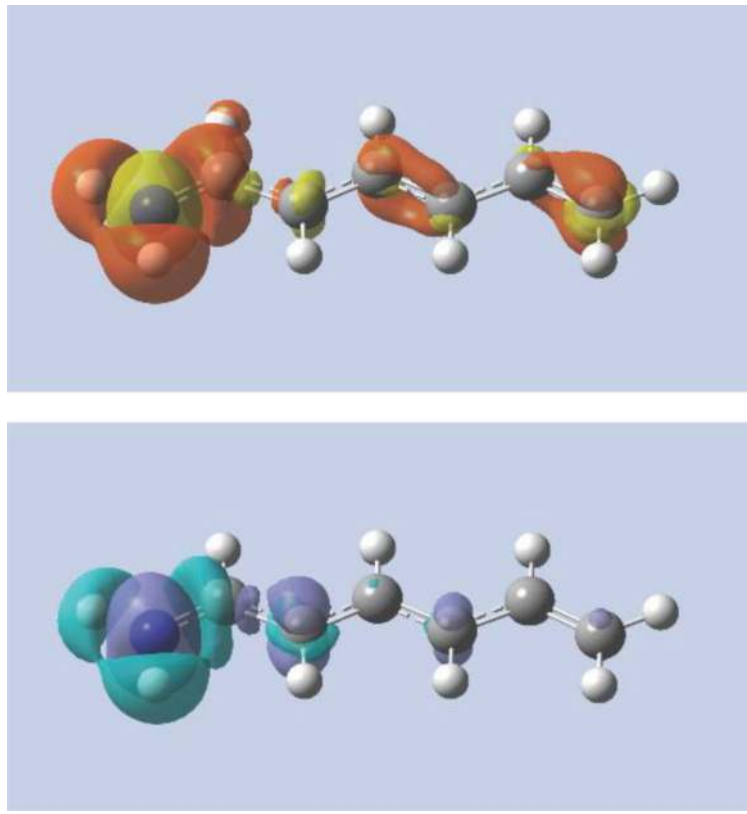

Figure 4. Alchemical change in density using the linear response (top) and softness kernel (bottom) for the heptatrienyl cation to 1,3,5-hexatriene-1-amine [38].

effect of functionalization dies off much more quickly under constant μ conditions. In fact, the third carbon atom is hardly affected in this—it should be stressed—unsaturated system, offering the possibility for mesomerism. In the LRF, the decay is slow and effects are still relatively important five bonds away from the perturbation.

Further case studies on '3D' systems (e.g. alchemically changing methylcubane to fluorocubane and on functionalized neopentane) yield similar results. All together, the results on the near-sightedness of the softness kernel found for all systems discussed in [38] are the first and a firm numerical confirmation of Kohn's NEM principle in the molecular world. To put it in chemical terms, these findings provide computational evidence for the transferability of functional groups: molecular systems can be divided into locally interacting subgroups retaining a similar functionality and reactivity that can only be influenced by changes in the direct environment of the functional group. Thus, the physicist's NEM principle and the chemist's transferability principle [45]—at the heart of, for example, the whole of organic chemistry [46]—are reconciled.

2.3. Extension of $\chi(\mathbf{r}, \mathbf{r}')$ in the context of spin polarized CDFT

As a natural extension of CDFT to the case where spin polarization is included [47–49], spin polarized conceptual DFT was introduced by Galvan et al. [50, 51] (see also Ghanty and Ghosh

[52] and for a review see [53]). In the so-called (N_α, N_β) representation, the response of the electronic energy to perturbations in the number of α electrons, N_α, the number of β electrons, N_β, the external potential acting on the α electrons, $v_\alpha(\mathbf{r})$, and the external potential acting on the β electrons, $v_\beta(\mathbf{r})$, is studied. In this representation, the $E = E[N, v]$ functional from Section 2.1 is generalized to the $E = E[N_\alpha, N_\beta, v_\alpha, v_\beta]$ functional. In the second, equivalent, (N, N_S) representation, in fact the one introduced by Galvan, the $E = E[N, v]$ functional is generalized to $E = E[N, N_S, v, v_S]$ or $E = E[N, N_S, v, \mathbf{B}]$ where N_S denotes the electron spin number defined as the difference between the number of α and β electrons, $N_S = N_\alpha - N_\beta$, whereas v_s is given by $v_S(\mathbf{r}) = (v_\alpha(\mathbf{r}) - v_\beta(\mathbf{r}))/2$.

$v(\mathbf{r})$ is equal to $(v_\alpha(\mathbf{r}) + v_\beta(\mathbf{r}))/2$ and $\mathbf{B}$ represents an external magnetic field. If the magnetic field is static and uniform along the z axis, one has $v_\alpha(\mathbf{r}) = v(\mathbf{r}) + \mu_B B_Z$ and $v_\beta(\mathbf{r}) = v(\mathbf{r}) - \mu_B B_Z$, $v(\mathbf{r})$ is the usual external spin-free potential (as used in CDFT without spin polarization), whereas $v_S(\mathbf{r})$ is related to the magnetic field $\mathbf{B}(\mathbf{r})$. In this context, and sticking to the (N, N_S) representation, three linear response functions can now be defined:

$$\chi_{NN}(\mathbf{r}, \mathbf{r}') = \left(\delta^2 E/\delta v(\mathbf{r})\delta v(\mathbf{r}')\right)_{N, N_S, v_S} \tag{27}$$

$$\chi_{SS}(\mathbf{r}, \mathbf{r}') = \left(\delta^2 E/\delta v_S(\mathbf{r})\delta v_S(\mathbf{r}')\right)_{N, N_S, v} \tag{28}$$

$$\begin{aligned}\chi_{NS}(\mathbf{r}, \mathbf{r}') &= \left(\delta^2 E/\delta v(\mathbf{r})\delta v_S(\mathbf{r}')\right)_{N, N_S} = (\delta\rho_N(\mathbf{r})/\delta v_S(\mathbf{r}'))_{N, N_S, v} \\ &= (\delta\rho_S(\mathbf{r}')/\delta v(\mathbf{r}))_{N, N_S, v} = \left(\delta^2 E/\delta v_S(\mathbf{r}')\delta v(\mathbf{r})\right)_{N, N_S} = \chi_{SN}(\mathbf{r}', \mathbf{r})\end{aligned} \tag{29}$$

where $\rho_N(\mathbf{r}) = \rho_\alpha(\mathbf{r}) + \rho_\beta(\mathbf{r})$ and $\rho_S(\mathbf{r}) = \rho_\alpha(\mathbf{r}) - \rho_\beta(\mathbf{r})$ are the total and spin densities, respectively. $\chi_{NN}(\mathbf{r}, \mathbf{r}')$ is the analogue of the spin-independent CDFT expression for the LRF $\chi(\mathbf{r}, \mathbf{r}')$ (Eq. (1)).

Space limitations prevent us to go in detail on the results reported in [47, 48]. We only depict in **Figure 5** the SPCDFT analogue of the contour plots for $\chi(\mathbf{r}, \mathbf{r}')$ for closed shell atoms as discussed in [47] and the Chem Soc Rev paper [16]. In **Figure 5**, we plot the LRF, in the (N_α, N_β) representation, for the ground state of Li ($(1s)^2\ (2s)^1$). The structure of $\chi_{\alpha\alpha}(\mathbf{r}, \mathbf{r}')$ and $\chi_{\beta\beta}(\mathbf{r}, \mathbf{r}')$ is similar to the $\chi(\mathbf{r}, \mathbf{r}')$ plots for closed shell atoms: a negative diagonal part (cfr [47] and Section 2.1) and alternating positive and negative parts for r or r′ = constant in order to obey the trivial equation (cf. [47])

$$\int \chi(\mathbf{r}, \mathbf{r}')d\mathbf{r} = \int (\delta\rho_N(\mathbf{r})/\delta v(\mathbf{r}'))_N d\mathbf{r} = (\delta N/\delta v(\mathbf{r}'))_N = 0 \tag{30}$$

$\chi_{\alpha\alpha}$ extends further away from the nucleus than $\chi_{\beta\beta}$ in line with the extra α electron with the higher principal quantum number (n = 2) extending farther away from the nucleus than the n = 1 β electron. $\chi_{\beta\beta}$ looks similar to the $\chi_{\beta\beta}$ plot for He (insert) but contracted more to the origin (due to higher nuclear charge). The $\chi_{\alpha\beta}$ and $\chi_{\alpha\beta}$ plots show some evident symmetry, $\chi_{\alpha\beta}(\mathbf{r}, \mathbf{r}') = \chi_{\beta\alpha}(\mathbf{r}', \mathbf{r})$, and show positive regions along the diagonal. A positive perturbation in

http://dx.doi.org/10.5772/intechopen.80280

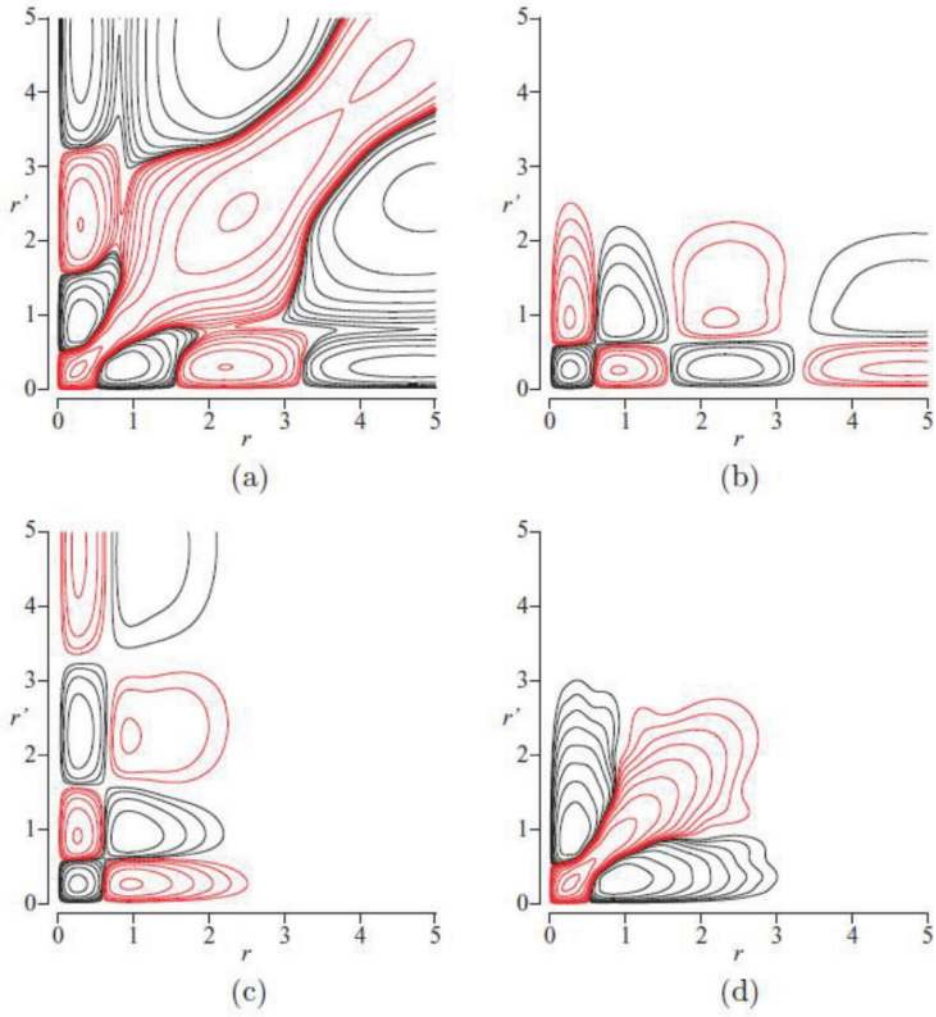

Figure 5. Contour plots of the radial distribution function of the spin polarized linear response function of Lithium in the [Nα, Nβ] representation. r is represented on the horizontal axis, r′ on the vertical axis [(a) Lithium $\chi_{\alpha\alpha}$, (b) Lithium $\chi_{\alpha\beta}$, (c) Lithium $\chi_{\alpha\alpha}$, (d) Lithium $\chi_{\beta\beta}$. In the insert, the $\chi_{\beta\beta}$ plot for He (see text) (Reprinted from [48] with the permission of AIP Publishing)].

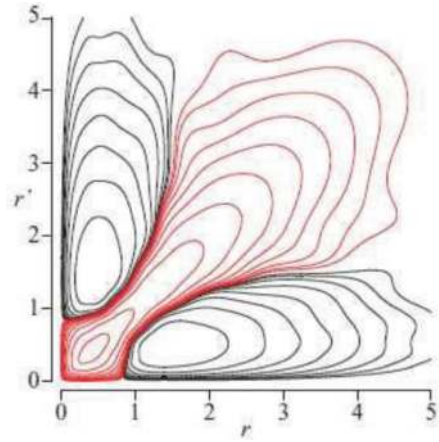

the α external potential $\delta v_\alpha(\mathbf{r})$ will cause a depletion of electrons in the vicinity of the perturbation, the β electrons are not affected directly. However, the depletion in α electrons will influence the Coulomb potential and due to the lower electron-electron repulsion, an accumulation in β electrons in the region considered will occur resulting in a positive diagonal $\chi_{\beta\alpha}(\mathbf{r},\mathbf{r})$ value. The concentration of the $\chi_{\alpha\beta}$ and $\chi_{\alpha\beta}$ isocontours along the r and r′ axes can be interpreted when referring to the $\chi_{\alpha\alpha}$ and $\chi_{\beta\beta}$ plots: perturbing $v_\beta(\mathbf{r})$ at a distance r′ larger than 3 a.u. clearly has no effect on the β density, the Coulomb potential, the overall density and consequently on the α density. This results in $\left(\delta\rho_\alpha(\mathbf{r})/\delta v_\beta(\mathbf{r}')\right) = \chi_{a\beta}(\mathbf{r},\mathbf{r}')$ having zero values for r′ larger than 3 a.u. On the other hand, perturbing $v_\beta(\mathbf{r})$ close to the nucleus induces a change in the β density, with repercussion on the Coulomb potential and so on the α density farther away from the nucleus (on the r axis) even in regions where the β density is no longer affected. All these features account for the 'partial plane filling' of the $\chi_{\alpha\beta}$ and $\chi_{\alpha\beta}$ plots with a 'demarcation' line at 3 a.u.

To close this section, we mention that once $\chi(\mathbf{r},\mathbf{r}')$ (or its counterparts in SPCDFT) is known, a local version of the polarizability tensor components, say α_{xy}, namely $\alpha_{xy}(\mathbf{r})$ can be obtained by straightforward integration:

$$\alpha_{xy}(\mathbf{r}) = -\int x(\mathbf{r})\chi(\mathbf{r},\mathbf{r}')y(\mathbf{r}')d\mathbf{r}' \tag{31}$$

An example is given in **Figure 6** [48] where for the atoms Li through Ne the trend of the spherically averaged $\alpha(\mathbf{r})$ $\left(\frac{1}{3}\left(\alpha_{xx}(\boldsymbol{r}) + \alpha_{yy}(\boldsymbol{r}) + \alpha_{zz}(\boldsymbol{r})\right)\right)$ is given. From 2 a.u. on, the trends in $\alpha(\mathbf{r})$ for Li up to Ne parallel the global polarizability, known to decrease along a period of the periodic table. At lower distances (preceding the valence region), inversions with even negative values occur. The present results are evidently important when, for example, disentangling reaction mechanisms where local polarizabilities, that is, in certain regions of the reagents, are

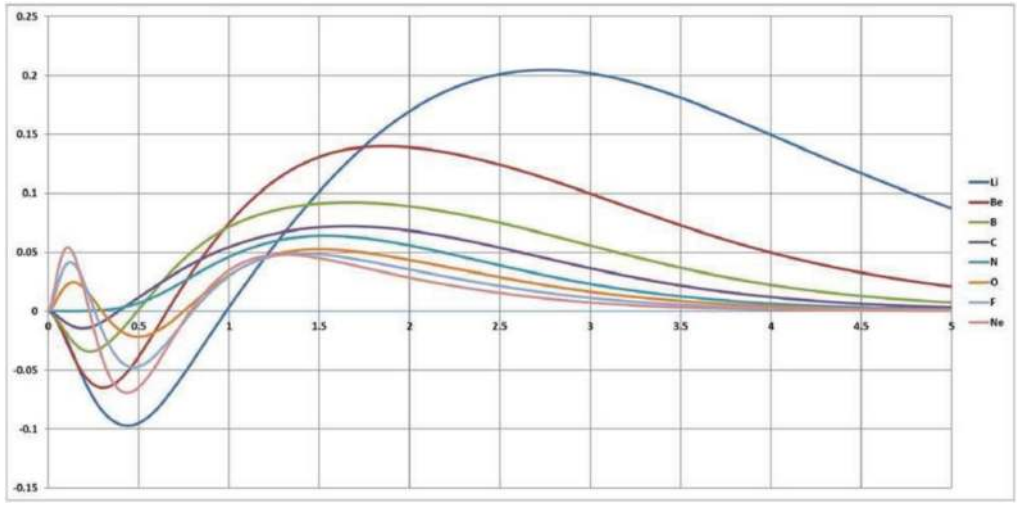

Figure 6. Plot of the local polarizability α(r) of the atoms Li through Ne via CPKS (see text) (Reprinted by permission of the publisher (Taylor and Francis Ltd.) [48]).

at stake and not the overall polarizability. The parallel between the relationship between local and global softness (Section 2.1) is obvious.

3. The role of the LRF in alchemical derivatives and exploring chemical compound space

3.1. Context

The LRF has recently been exploited when investigating Chemical Compound Space [54–56]. Chemists are continuously exploring chemical compound space (CCS) [57, 58], the space populated by all imaginable chemicals with natural nuclear charges and realistic interatomic distances for which chemical interactions exist. Navigating through this space is costly, obviously for synthetic-experimental chemists and also for theoretical and computational chemists who might and should be guides for indicating relevant domains in CCS to their experimental colleagues. Doing even a simple single-point SCF calculation at every imaginable point leads to prohibitively large computing times (not to speak about bookkeeping aspects and manipulation of the computed data). A very promising ansatz was initiated by Von Lilienfeld et al. [59–63] in his alchemical coupling approach where two, isoelectronic molecules in CCS are coupled 'alchemically' through the interpolation of their external potentials (see also the work by Yang and co-workers on designing molecules by optimizing potentials [64]). At the heart of this ansatz are the alchemical derivatives, partial derivatives of the energy w.r.t. one or more nuclear charges at constant number of electrons and geometry. The simplest members of this new family of response functions are:

the alchemical potential

$$\mu_A^{\mathrm{al}}[N,\mathbf{Z},\mathbf{R}] \equiv (\partial W/\partial Z_A)_{\mathcal{N},\mathbf{R}} = (\partial E/\partial Z_A)_{\mathcal{N},\mathbf{R}} + (\partial V_{\mathrm{nn}}/\partial Z_A)_{\mathcal{N},\mathbf{R}} = \mu_A^{\mathrm{al,el}} + \mu_A^{\mathrm{al,nuc}} \tag{32}$$

and the alchemical hardness

$$\eta_{AB}^{\mathrm{al}}[N,\mathbf{Z},\mathbf{R}] \equiv \left(\partial^2 W/\partial Z_A \partial Z_B\right)_{\mathcal{N},\mathbf{R}} = \left(\partial^2 E/\partial Z_A \partial Z_B\right)_{\mathcal{N},\mathbf{R}} + \left(\partial^2 V_{\mathrm{nn}}/\partial Z_A \partial Z_B\right)_{\mathcal{N},\mathbf{R}} = \eta_{AB}^{\mathrm{al,el}} + \eta_{AB}^{\mathrm{al,nuc}} = \eta_{BA}^{\mathrm{al}}, \tag{33}$$

where $W[N,\mathbf{Z},\mathbf{R}] \equiv E[N,v[\mathbf{Z},\mathbf{R}]] + V_{\mathrm{nn}}[\mathbf{Z},\mathbf{R}]$ is the total energy of a system,$\mathbf{R} = (\mathbf{R}_A,\mathbf{R}_B,\ldots)$ denotes constant geometry and $\mathbf{Z} = (Z_A,Z_B,\ldots,)$denotes the nuclear charges vector. The analogy with the electronic chemical potential and hardness (see Section 1) is striking. Some years ago, one of the present authors (R.B.) presented a strategy to calculate these derivatives for any atom or atom-atom combination analytically and to use them, starting from a single SCF calculation on the parent or reference molecule, to explore the CCS of first neighbours, implying changes of nuclear charges of +1 or −1 [65]. In this way, simple arithmetic can be used, starting from a Taylor expansion

$$\Delta W[d\mathbf{Z}] = W[N,\mathbf{Z}+d\mathbf{Z},\mathbf{R}] - W[N,\mathbf{Z},\mathbf{R}] = \sum_A \mu_A^{\mathrm{al}} dZ_A + 1/2 \sum_A \sum_B \eta_{AB}^{\mathrm{al}} dZ_A dZ_B \tag{34}$$

instead of a new SCF calculation for each transmutant.

The position of the alchemical derivatives in CDFT was already mentioned: they are response functions, now related to a particular charge in external potential, namely the charge in one or more nuclear charges. As the second derivatives are 'diagonal' in these particular external potential changes, a direct link with the LRF can be expected. Using the chain rule, one easily writes

$$\begin{aligned}\eta_{AB}^{\mathrm{al,el}} = \left(\partial^2 E[N, v[\mathbf{Z}, \mathbf{R}]]/\partial Z_A \partial Z_B\right)_{N,\mathbf{R}} &= \int\int (\delta\rho(\mathbf{r})/\delta v(\mathbf{r}'))_N (\partial v(\mathbf{r})/\partial Z_A)_{N,\mathbf{R}} (\partial v(\mathbf{r}')/\partial Z_B)_{N,\mathbf{R}} d\mathbf{r} d\mathbf{r}' \\ &= \int\int \chi(\mathbf{r}, \mathbf{r}')(1/|\mathbf{r} - \mathbf{R}_A|)(1/|\mathbf{r}' - \mathbf{R}_B|) d\mathbf{r} d\mathbf{r}'\end{aligned} \tag{35}$$

indicating that the alchemical hardness is obtained by integration of the LRF after multiplication by $1/|\mathbf{r} - \mathbf{R}_A|$ and $1/|\mathbf{r}' - \mathbf{R}_B|$. The basic relationship of the alchemical derivatives and the LRF shows how, again, the LRF makes its appearance in sometimes unexpected areas (see also Section 4). In the case of the first derivative, the $(\delta E/\delta v(\mathbf{r}))_N$ factor in the integrand simplifies to $\rho(\mathbf{r})$(see Section 1), yielding.

$$\mu_A^{\mathrm{al,el}} = \int \rho(\mathbf{r})/|\mathbf{r} - \mathbf{R}_A| d\mathbf{r} \tag{36}$$

the electronic potential at the nucleus, well known as the electronic part of the molecular electrostatic potential [66].

3.2. Applications

As a very simple example, we consider the transmutation of the nitrogen molecule. Five chemically relevant mutants can be generated (see **Figure 7**) as nearest neighbours in CCS ($\Delta Z = \pm 1$) and at constant number of electrons: CO, NO^+, O_2^{2+}, CN^- and C_2^{2-}. The differences between 'vertical' (i.e. exact, via two SCF calculations) and alchemical transmutation energies were evaluated at the B3LYP/cc-pCVTZ level (note the inclusion of additional tight functions 'C in

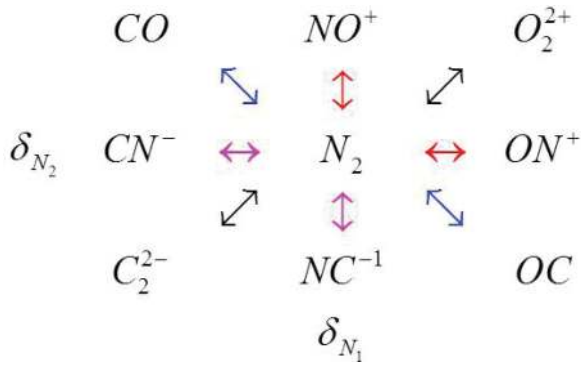

Figure 7. Transmutation of the nitrogen molecule to its nearest neighbours in chemical compound space (Reprinted with permission from [54]. Copyright (2017) American Chemical Society).

order to recover the (changes in) core-core and core-valence correlation). The mean absolute error was only 0.034 a.u., the $N_2 \rightarrow CO$transmutation being particularly successful with a difference in energy of only 0.004 a.u., that is, 2 kcal mol $^{-1}$. The transmutation into a neutral system results in the cancellation of the odd terms in the Taylor expansion. Of course, we do not claim 'chemical accuracy', yet the ordering of the energy of all transmutants came out correctly, indicating that the alchemical procedure (even when stopped at second order) is a simple, straightforward road to explore CCS for neighbouring structures.

Similar conclusions could be drawn for transmutation of benzene, for example, by the substitution of CC units by their isoelectronic BN units. The replacement of a CC unit in an aromatic molecule by an isoelectronic unit BN has been shown to impart important, interesting electronic, photophysical and chemical properties, often distinct from the parent hydrocarbon [67]. An in-depth study of all azoborines (**Figure 8**) $C_6H_6 \rightarrow C_{6\text{-}2n}H_6(BN)_n$ ($n = 1, 2, 3$) turned out to reproduce correctly the stability of all possible isomers for a given n value (3,11,3 for $n = 1, 2, 3$), which is of importance for applications in graphene chemistry where the $(CC)_n \rightarrow (BN)_n$ substitution is a topic that has received great interest in recent years [68].

As a computational 'tour de force' , and passing from '2D' benzene to '3D' fullerenes, we recently explored the alchemical approach to study the complete $(CC)_n \rightarrow (BN)_n$ substitution pattern of C_{60}, all the way down to $(BN)_{30}$. $C_{60} \rightarrow C_{60\text{-}2n}(BN)_n$, $n = 1, 2, \ldots, 30$, predicting and interpreting via 'alchemical rules' the most stable isomers for each value of n. This study is based on a *single* SCF calculation on C_{60} and its alchemical derivatives up to second order, enabling each possible transmutation energy to be evaluated by simple arithmetic (the diagonal elements of the alchemical hardness matrix are equal)

$$\Delta W_n[\mathbf{N} = (N1, \ldots, Nn), \mathbf{B} = (B1, \ldots, Bn)] = n\,\eta^{\mathrm{al}}_{11} + \sum_{i=1}\sum_{j>i}\left(\eta^{\mathrm{al}}_{\mathrm{N}i\mathrm{N}j} + \eta^{\mathrm{al}}_{\mathrm{B}i\mathrm{B}j}\right) - \sum_{i=1}\sum_{j=1}\eta^{\mathrm{al}}_{\mathrm{N}i\mathrm{B}j}, \tag{37}$$

where ΔW_n is the transmutation energy from C_{60} to $C_{60\text{-}2n}(BN)_n$ and $\mathbf{N}/\mathbf{B}$ is a vector of the carbon atoms replaced by the nitrogen/boron atoms.

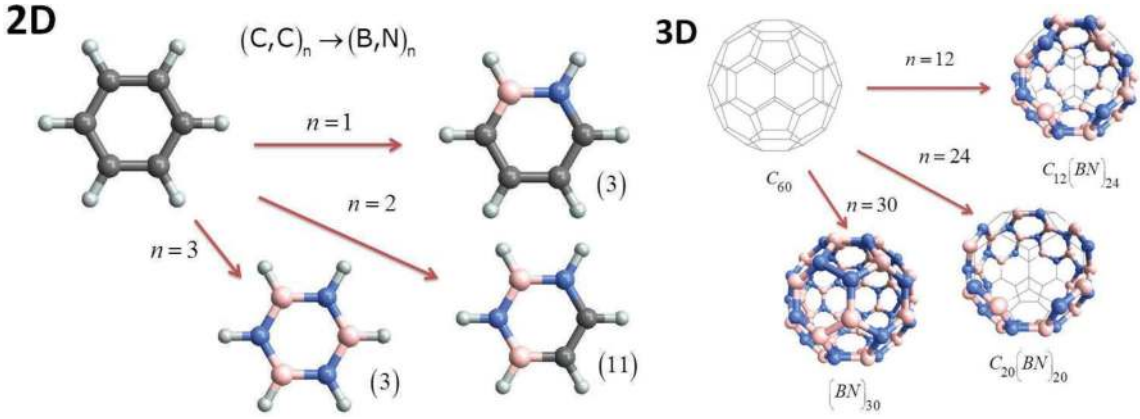

Figure 8. CC-BN Substitutions in 2D and 3D unsaturated carbocyclic systems (number of isomers for the 2D case in parentheses).

In (37), it is seen that the linear term drops as μ_i is unique by symmetry for all atoms in C_{60} and because $\Sigma\ \Delta Z_i = 0$ for any transmutation. The alchemical hardness matrix $\boldsymbol{\eta}$ thus completely determines the substitution energy and pattern. To summarize the results (for an in-depth discussion see [55]), the study reveals that the correct sequence of stabilization energies for each n is retrieved by adopting an approach in which for each n value the problem is looked upon without prejudice of the $n - 1$ result (called the 'simultaneous' approach). The other, simpler method (we called it the 'successive' approach) was shown to fail already after n = 13, be it that at some n values identical values were obtained with both approaches, for example, for the Belt structure (n = 20). Needless to say that even the 'successive' approach might already be prohibitively demanding for standard ab initio or DFT calculations, let it be for the simultaneous method. The sequence of substitutions could be interpreted in terms of a number of 'alchemical' rules of which the two most important are when (referring to earlier work by Kar et al. [69]): (1°) hexagon-hexagon junctions are preferably substituted, in a way that minimizes the homonuclear (BB,NN) bonds and (2°) the higher stability is created by maximizing the number of filled hexagons. For the subsequent, more intricate, rules we refer to [55].

Shortage of space prevents us to comment on our recent results on the evaluation of isolated atom alchemical derivatives up to third order with different techniques, from numerical differentiation (not discussed hitherto in this chapter), via the coupled perturbed Kohn-Sham approach as discussed before, to the March and Parr combined $1/Z$ and $N^{-1/3}E[N, Z]$ expansion ansatz [70], permitting a walk through the periodic table on the road to scrutinize periodicity effects [56].

4. The role of the LRF (or its forerunner, the atom-atom polarizability) in evaluating and interpreting molecular electronics

4.1. Context

In this section the role of the LRF in molecular electronics is highlighted [72] has been a vibrant area of research in recent years. An ever-increasing number of papers (both experimental and theoretical) studied the transport properties of typically organic molecules containing π-conjugated systems and considering possible applications for incorporation in molecular electronic devices (MED) [73]. Most of these theoretical studies have been performed at a high level of theory, but this type of calculation does not always lead to simple insights into why some molecules will conduct and which will insulate, and how the positions of the contacts influence this behaviour.

We therefore adopted a simple ansatz based on Ernzerhof's source and sink potential (for details see [74, 75]) in Fowler's tight-binding Hückel approach [76]. One thereby considers only the π electrons of the molecule and cuts the resonance effects between the contact and the molecule after the molecule's nearest neighbour in the contact. In the so-called weak interaction limit (see details in [71]), the transmission probability at the Fermi level $T(0)$, which is directly proportional to the conductance, can then be written as

$$T(0) = 4\beta^2\Delta_{AB}^2/\Delta^2 \tag{38}$$

Here, as in Section 2.1, Δ is the Hückel determinant for the isolated molecule, from which in Δ_{AB} its A-th row and B-th column are deleted and β is a measure of the interaction between the contact atom and its molecular neighbour. Again, what is the role of the LRF in this road to calculating/understanding molecular conductivity?

4.2. The atom-atom polarizability as a conductivity indicator

Going back to expression (7) for the diagonal elements of Coulson's atom-atom polarizability, a general element π_{AB} of this forerunner of the LRF can be written as

$$\pi_{AB} = (1/\pi) \int_{-\infty}^{+\infty} (\Delta_{AB}(iy)/\Delta(iy))^2 dy \tag{39}$$

(the contour integral in the complex plane in Coulson's formalism [31] is hereby reduced to an integral along the imaginary axis). The integrand of π_{AB} thus turns out to be related to the transition probability at the Fermi level T_r $T_{AB}(0)$ when the contacts are placed at atoms A and B of the molecule. An intimate relation between π_{AB} and $T_{AB}(0)$ thus exists; the precise connection was evaluated by explicit calculation of π_{AB} and $T_{AB}(0)$, some results being visualized in **Figure 9**. There, we depict both the π_{AB} and $T_{AB}(0)$ values for some linear acenes (benzene, naphthalene, anthracene and tetracene), taking always one atom as the reference atom. For the atom-atom polarizability, the reference atom is denoted by a green circle with its area proportional to the self-polarizability of that atom which is as pointed out in Section 2.1 as always negative. Black and red circles on the other atoms denote the atom-atom polarizability values corresponding to a perturbation on the reference atom (varying α_A) on the (charge of the) considered atom $B(q_B)$. Black circles correspond to $\pi_{AB} > 0$, red circles to $\pi_{AB} < 0$. For $T_{AB}(0)$, a similar approach is followed. The empty green circle denotes the position of the first contact 'A' (zero 'ipso' transmission [71]), the magnitude of the black circles on the other atoms 'B' denotes the magnitude of the transmission when the second contact is placed at position B; note that no red circles arise as $T_{AB}(0)$, the transmission probability, always lies between 0 and 1.

Figure 9 shows that the pattern in the two plots is completely analogous and leads to the conjecture that a positive atom-atom polarizability seems to be a necessary condition in these Kekulean benzenoids in order to have transmission for a certain configuration of the contacts on the molecule. If the areas of the circles are considered, no exact proportionality between π_{AB} and $T_{AB}(0)$ can be inferred, but they are correlated.

This issue was further investigated in the next linear acene and pentacene (**Figure 10**), by varying the position of the first contact. For a fixed first contact, the highest transmission occurs when the second contact is at the atom with the highest π_{AB} value involving the first atom. From that atom on, a monotonously decreasing probability is noticed in either directions. The sharpest decline in T is in the direction of the neighbour that exhibits the lowest atom-atom polarizability. On the basis of these results, it can indeed be conjectured that a positive atom-atom polarizability is a necessary condition for transmission and that the tendencies between the two series of values are similar.

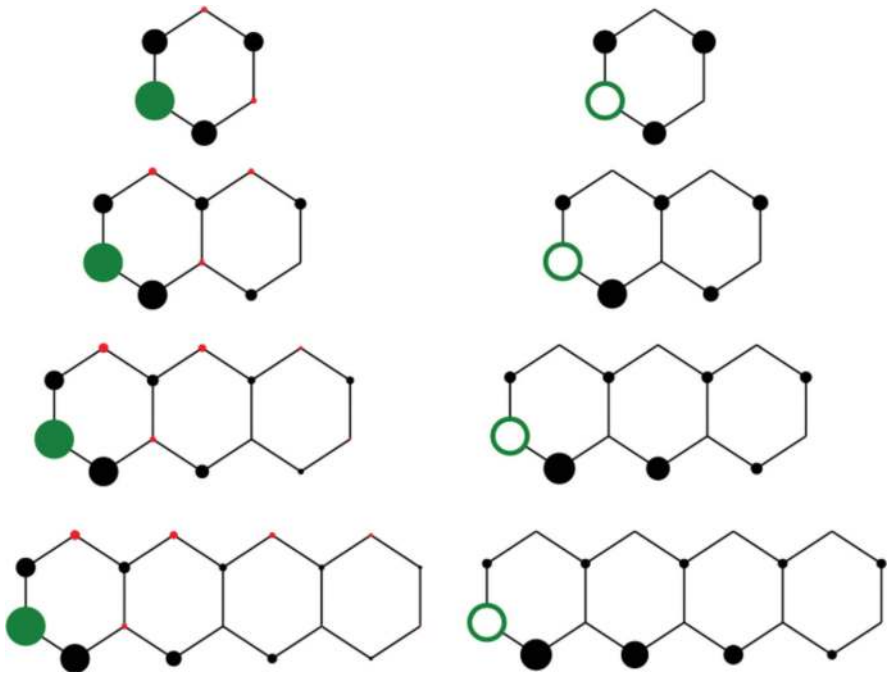

Figure 9. The atom-atom polarizability (left) and transmission probability at the Fermi level (right) for a single reference atom for benzene, naphthalene, anthracene and tetracene (Reprinted from [71] with permission of AIP Publishing).

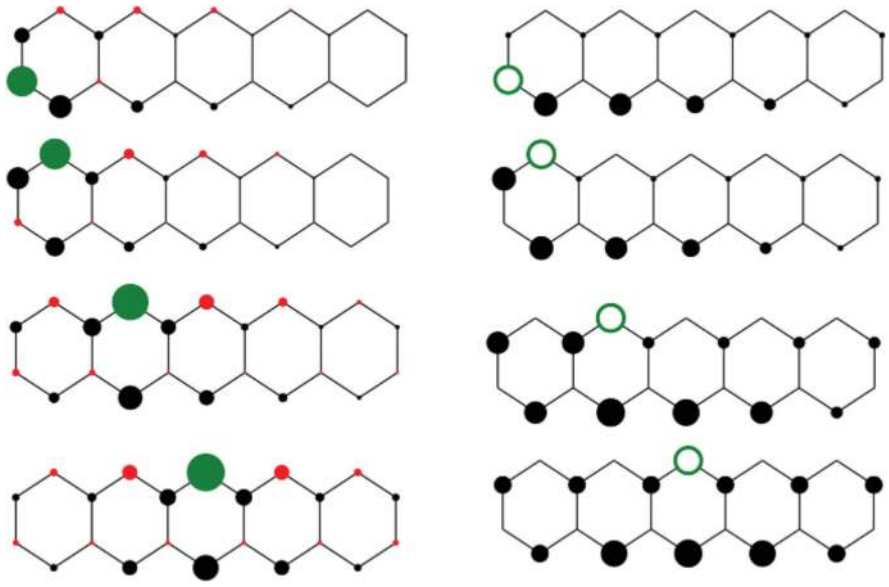

Figure 10. The atom-atom polarizability (left) and transmission probability at the Fermi level (right) for pentacene for variable reference atom (Reprinted from [71] with permission of AIP Publishing).

Further analysis of the behaviour of the $(\Delta_{AB}/\Delta)^2$ function in the complex plane was done in the case of alternant non-singular hydrocarbons (for details see [71]). Coulson's and Longuet Higgins' pairing theorem shows that if A and B are drawn from the same partite set (all 'starred' or 'unstarred' atoms, respectively) $\Delta^2_{\mathrm{AB}}(z)/\Delta\,(z)^2$ is odd and if A and B are taken from

a different set this function is even. It is then easily seen that the odd function has no real part along the imaginary axis, leading to a negative $(\Delta_{AB}/\Delta)^2$ value along the y axis and zero at the origin, yielding a negative atom-atom polarizability and zero transmission at the Fermi level ($T(0)$). On the other hand, when A and B are drawn from opposite sets, Δ_{AB}/Δ is an even function yielding real values along the y axis. A positive π_{AB} value results with either insulation or transmission, depending on whether $\Delta_{AB}(0)$ is zero or not. Note that the analysis for $A = B$ leads to the same result as for $A \neq B$ but belonging to the same set yielding a negative π_{AA} value. The following overall conclusion, formulated as a selection rule, can be drawn: negative atom-atom polarizabilities for non-singular alternant hydrocarbons correspond to devices with insulation at the Fermi level. Conduction at the Fermi level requires, but is not guaranteed by, a positive atom-atom polarizability.

The aforementioned properties were used as guiding principle in our later studies towards a chemical interpretation of molecular electronic conductivity [77] leading to a simple, back-of-the-envelope determination of quantum interference [78], thus bridging the gap between chemical reactivity theory and molecular electronics.

5. Conclusions

The LRF and its congener, the softness kernel, are now in a stage where many of their mathematical and physical properties are well understood. The possibility to evaluate, represent and interpret them puts them on equal footing for their use in conceptual DFT with their already more traditional second-order companions, the chemical hardness and the Fukui function. In view of the 'chemistry' contained in the LRF kernel as shown some years ago, it is not unexpected, but it still remains to be unravelled whether they are major players in very fundamental issues pertaining to the electronic structure of matter as in Kohn's nearsightedness of electronic matter principle, as well as in more applied fields where they are shown to be of great use to explore chemical compound space (through the alchemical derivatives) and to predict/interpret molecular conductivity.

Acknowledgements

P.G. and F.D.P. acknowledge the Vrije Universiteit Brussel (VUB) for a Strategic Research Program. F.D.P. also acknowledges the Franqui Foundation for a position as Francqui Research Professor. S.F. acknowledges the Research Foundation Flanders (FWO) and the European Union's Horizon 2020 Marie Sklodowska-Curie grant (N° 706415) for financially supporting his postdoctoral research at the ALGC group. T.S. acknowledges the FWO for a position as research assistant (11ZG615N). P.W.A. thanks the Natural Sciences and Engineering Research Council, the Canada Research Chairs and Compute Canada for financial support. R.B. thanks the Interdisciplinary Centre for Mathematical and Computational Modelling for a computing grant. P.G. thanks Kristina Nikolova for her meticulous help in styling the manuscript and Tom Bettens for his help in styling **Figure 2**.

Conflicts of interest

.The authors report no conflicts of interest regarding this publication.

Author details

Paul Geerlings[1]*, Stijn Fias[1,2], Thijs Stuyver[1], Paul Ayers[2], Robert Balawender[3] and Frank De Proft[1]

*Address all correspondence to: pgeerlin@vub.be

1 Algemene Chemie, Vrije Universiteit Brussel, Brussels, Belgium

2 Department of Chemistry and Chemical Biology, McMaster University, Hamilton, ON, Canada

3 Institute of Physical Chemistry, Polish Academy of Sciences, Warsaw, Poland

References

[1] Parr RG, Yang W. Density-functional theory of the electronic structure of molecules. Annual Review of Physical Chemistry. 1995;**46**:701-728. DOI: 10.1146/annurev.pc.46.100195.003413

[2] Chermette H. Chemical reactivity indexes in density functional theory. Journal of Computational Chemistry. 1999;**20**:129-154. DOI: 10.1002/(SICI)1096-987X(19990115)20:1<129::AID-JCC13>3.3.CO;2-1

[3] Geerlings P, De Proft F, Langenaeker W. Conceptual density functional theory. Chemical Reviews. 2003;**103**:1793-1874. DOI: 10.1021/cr990029p

[4] Ayers PW, Anderson JSM, Bartolotti LJ. Perturbative perspectives on the chemical reaction prediction problem. International Journal of Quantum Chemistry. 2005;**101**:520-534. DOI: 10.1002/qua.20307

[5] Gázquez JL. Perspectives on the density functional theory of chemical reactivity. Journal of the Mexican Chemical Society. 2008;**52**:3-10

[6] Liu SB. Conceptual density functional theory and some recent developments. Acta Physico-Chimica Sinica. 2009;**25**:590-600. DOI: 10.3866/PKU.WHXB20090332

[7] Hohenberg P, Kohn W. Inhomogeneous electron gas. Physical Review. 1964;**136**:B864-B871. DOI: 10.1103/PhysRev.136.B864

[8] Parr RG, Weitao Y. Density-Functional Theory of Atoms and Molecules. International Series of Monographs on Chemistry. London/New York: Oxford University Press; 1989

[9] Sanderson RT. An interpretation of bond lengths and a classification of bonds. Science. 1951;**114**:670-672. DOI: 10.1126/science.114.2973.670

[10] Pearson RG. Hard and soft acids and bases. Journal of the American Chemical Society. 1963;**85**:3533-3539. DOI: 10.1021/ja00905a001

[11] Parr RG, Donnelly RA, Levy M, Palke WE. Electronegativity: The density functional viewpoint. The Journal of Chemical Physics. 1978;**68**:3801-3807. DOI: 10.1063/1.436185

[12] Parr RG, Pearson RG. Absolute hardness: Companion parameter to absolute electronegativity. Journal of the American Chemical Society. 1983;**105**:7512-7516. DOI: 10.1021/ja00364a005

[13] Parr RG, Yang W. Density functional approach to the frontier-electron theory of chemical reactivity. Journal of the American Chemical Society. 1984;**106**:4049-4050. DOI: 10.1021/ja00326a036

[14] Geerlings P, De Proft F. Conceptual DFT: The chemical relevance of higher response functions. Physical Chemistry Chemical Physics. 2008;**10**:3028. DOI: 10.1039/b717671f

[15] Morell C, Grand A, Toro-Labbé A. New dual descriptor for chemical reactivity. The Journal of Physical Chemistry. A. 2005;**109**:205-212. DOI: 10.1021/jp046577a

[16] Geerlings P, Fias S, Boisdenghien Z, De Proft F. Conceptual DFT: Chemistry from the linear response function. Chemical Society Reviews. 2014;**43**:4989. DOI: 10.1039/c3cs60456j

[17] Runge E, Gross EKU. Density-functional theory for time-dependent systems. Physical Review Letters. 1984;**52**:997-1000. DOI: 10.1103/PhysRevLett.52.997

[18] Marques MAL, Ullrich CA, Nogueira F, Rubio A, Burke K, Gross EKU. Time-Dependent Density Functional Theory. Lecture Notes in Physics. Vol. 706. Berlin, Heidelberg: Springer; 2006. DOI: 10.1007/b11767107

[19] Marques MAL, Maitra NT, Nogueira FMS, Gross EKU, Rubio A. Fundamentals of Time-Dependent Density Functional Theory. Lecture Notes in Physics. Vol. 837. Berlin, Heidelberg: Springer; 2012. DOI: 10.1007/978-3-642-23518-4

[20] Casida ME. Time-dependent density functional response theory for molecules. In: Recent Advances in Density Functional Methods. Singapore: World Scientific; 1995. pp. 155-192. DOI: 10.1142/9789812830586_0005

[21] Ayers PW. Strategies for computing chemical reactivity indices. Theoretical Chemistry Accounts. 2001;**106**:271-279. DOI: 10.1007/PL00012385

[22] Geerlings P, Boisdenghien Z, De Proft F, Fias S. The E = E[N, v] functional and the linear response function: A conceptual DFT viewpoint. Theoretical Chemistry Accounts. 2016;**135**:213. DOI: 10.1007/s00214-016-1967-9

[23] Geerlings P, De Proft F, Fias S. Analogies between density functional theory response kernels and derivatives of thermodynamic state functions. Acta Physico-Chimica Sinica. 2018;**34**:699-707

[24] Perdew JP, Parr RG, Levy M, Balduz JL. Density-functional theory for fractional particle number: Derivative discontinuities of the energy. Physical Review Letters. 1982;**49**:1691-1694. DOI: 10.1103/PhysRevLett.49.1691

[25] Lieb EH. Density functionals for Coulomb systems. International Journal of Quantum Chemistry. 1983;**24**:243-277. DOI: 10.1002/qua.560240302

[26] Eschrig H. The Fundamentals of Density Functional Theory. Stuttgart-Leipzig, Germany: Teubner; 1996

[27] Kvaal S, Ekström U, Teale AM, Helgaker T. Differentiable but exact formulation of density-functional theory. Journal of Chemical Physics. 2014;**140**:18A518. DOI: 10.1063/1.4867005

[28] Helgaker T. In: 13th Sostrup Summer School on Quantum Chemistry and Molecular Properties; 2014

[29] Sablon N, De Proft F, Ayers PW, Geerlings P. Computing second-order functional derivatives with respect to the external potential. Journal of Chemical Theory and Computation. 2010;**6**:3671-3680. DOI: 10.1021/ct1004577

[30] Boisdenghien Z, Van Alsenoy C, De Proft F, Geerlings P. Evaluating and interpreting the chemical relevance of the linear response kernel for atoms. Journal of Chemical Theory and Computation. 2013;**9**:1007-1015. DOI: 10.1021/ct300861r

[31] Coulson CA, Longuet-Higgins HC. The electronic structure of conjugated systems. I. General theory. Proceedings of the Royal Society of London. Series A: Mathematical and Physical Sciences. 1947;**191**:39-60. DOI: 10.1098/rspa.1947.0102

[32] Nalewajski RF, Parr RG. Legendre transforms and Maxwell relations in density functional theory. The Journal of Chemical Physics. 1982;**77**:399-407. DOI: 10.1063/1.443620

[33] Callen HB. Thermodynamics and an Introduction to Thermostatistics. New York, USA: Wiley; 1985

[34] Berkowitz M, Parr RG. Molecular hardness and softness, local hardness and softness, hardness and softness kernels, and relations among these quantities. The Journal of Chemical Physics. 1988;**88**:2554-2557. DOI: 10.1063/1.454034

[35] Prigogine I, Defay R. Chemical Thermodynamics. London, UK: Longmans; 1954

[36] Berry RS, Rice SA, Ross J. Physical Chemistry. New York, USA: John Wiley & Sons; 1980

[37] Yang W, Parr RG. Hardness, softness, and the Fukui function in the electronic theory of metals and catalysis. Proceedings of the National Academy of Sciences. 1985;**82**:6723-6726. DOI: 10.1073/pnas.82.20.6723

[38] Fias S, Heidar-Zadeh F, Geerlings P, Ayers PW. Chemical transferability of functional groups follows from the nearsightedness of electronic matter. Proceedings of the National Academy of Sciences. 2017;**114**:11633-11638. DOI: 10.1073/pnas.1615053114

[39] Kohn W. Density functional and density matrix method scaling linearly with the number of atoms. Physical Review Letters. 1996;**76**:3168-3171. DOI: 10.1103/PhysRevLett.76.3168

[40] Prodan E, Kohn W. Nearsightedness of electronic matter. Proceedings of the National Academy of Sciences. 2005;**102**:11635-11638. DOI: 10.1073/pnas.0505436102

[41] Yang W, Cohen AJ, De Proft F, Geerlings P. Analytical evaluation of Fukui functions and real-space linear response function. The Journal of Chemical Physics. 2012;**136**:144110. DOI: 10.1063/1.3701562

[42] Sablon N, De Proft F, Geerlings P. The linear response kernel: Inductive and resonance effects quantified. Journal of Physical Chemistry Letters. 2010;**1**:1228-1234. DOI: 10.1021/jz1002132

[43] Cárdenas C, Rabi N, Ayers PW, Morell C, Jaramillo P, Fuentealba P. Chemical reactivity descriptors for ambiphilic reagents: Dual descriptor, local hypersoftness, and electrostatic potential. The Journal of Physical Chemistry. A. 2009;**113**:8660-8667. DOI: 10.1021/jp902792n

[44] Cárdenas C, Echegaray E, Chakraborty D, Anderson JSM, Ayers PW. Relationships between the third-order reactivity indicators in chemical density-functional theory. The Journal of Chemical Physics. 2009;**130**:244105. DOI: 10.1063/1.3151599

[45] Bader RFW. Nearsightedness of electronic matter as seen by a physicist and a chemist. The Journal of Physical Chemistry. A. 2008;**112**:13717-13728. DOI: 10.1021/jp806282j

[46] Patai S. PATAI's chemistry of functional groups. Wiley Online. DOI: 10.1002/SERIES1078

[47] Boisdenghien Z, Fias S, Van Alsenoy C, De Proft F, Geerlings P. Evaluating and interpreting the chemical relevance of the linear response kernel for atoms II: Open shell. Physical Chemistry Chemical Physics. 2014;**16**:14624. DOI: 10.1039/c4cp01331j

[48] Fias S, Boisdenghien Z, De Proft F, Geerlings P. The spin polarized linear response from density functional theory: Theory and application to atoms. The Journal of Chemical Physics. 2014;**141**:184107. DOI: 10.1063/1.4900513

[49] Boisdenghien Z, Fias S, Da Pieve F, De Proft F, Geerlings P. The polarizability of atoms and molecules: A comparison between a conceptual density functional theory approach and time-dependent density functional theory. Molecular Physics. 2015;**113**:1890-1898. DOI: 10.1080/00268976.2015.1021110

[50] Galván M, Gázquez JL, Vela A. Fukui function: Spin-density and chemical reactivity. The Journal of Chemical Physics. 1986;**85**:2337-2338. DOI: 10.1063/1.451083

[51] Galvan M, Vela A, Gazquez JL. Chemical reactivity in spin-polarized density functional theory. The Journal of Physical Chemistry. 1988;**92**:6470-6474. DOI: 10.1021/j100333a056

[52] Ghanty TK, Ghosh SK. Spin-polarized generalization of the concepts of electronegativity and hardness and the description of chemical binding. Journal of the American Chemical Society. 1994;**116**:3943-3948. DOI: 10.1021/ja00088a033

[53] De Proft F, Chamorro E, Pérez P, Duque M, De Vleeschouwer F, Geerlings P. Spin-polarized reactivity indices from density functional theory: Theory and applications. Chemical Modelling. 2009;**6**:63-111. DOI: 10.1039/b812888j. Cambridge: Royal Society of Chemistry

[54] Balawender R, Welearegay MA, Lesiuk M, De Proft F, Geerlings P. Exploring chemical space with the alchemical derivatives. Journal of Chemical Theory and Computation. 2013;**9**:5327-5340. DOI: 10.1021/ct400706g

[55] Balawender R, Lesiuk M, De Proft F, Geerlings P. Exploring chemical space with alchemical derivatives: BN-simultaneous substitution patterns in C 60. Journal of Chemical Theory and Computation. 2018;**14**:1154-1168. DOI: 10.1021/acs.jctc.7b01114

[56] Balawender R, Holas A, De Proft F, Van Alsenoy C, Geerlings P. Alchemical Derivatives of Atoms: A Walk Through the Periodic Table. Many-body Approaches at Different Scales. Cham, Switzerland: Springer International Publishing; 2018. pp. 227-251. DOI: 10.1007/978-3-319-72374-7_20

[57] Kirkpatrick P, Ellis C. Chemical space. Nature. 2004;**432**:823-823. DOI: 10.1038/432823a

[58] Dobson CM. Chemical space and biology. Nature. 2004;**432**:824-828. DOI: 10.1038/nature03192

[59] von Lilienfeld OA, Tuckerman ME. Molecular grand-canonical ensemble density functional theory and exploration of chemical space. The Journal of Chemical Physics. 2006;**125**:154104. DOI: 10.1063/1.2338537

[60] von Lilienfeld OA, Tuckerman ME. Alchemical variations of intermolecular energies according to molecular grand-canonical ensemble density functional theory. Journal of Chemical Theory and Computation. 2007;**3**:1083-1090. DOI: 10.1021/ct700002c

[61] von Lilienfeld OA. Accurate ab initio energy gradients in chemical compound space. The Journal of Chemical Physics. 2009;**131**:164102. DOI: 10.1063/1.3249969

[62] von Lilienfeld OA. First principles view on chemical compound space: Gaining rigorous atomistic control of molecular properties. International Journal of Quantum Chemistry. 2013;**113**:1676-1689. DOI: 10.1002/qua.24375

[63] Chang KYS, Fias S, Ramakrishnan R, von Lilienfeld OA. Fast and accurate predictions of covalent bonds in chemical space. The Journal of Chemical Physics. 2016;**144**:174110. DOI: 10.1063/1.4947217

[64] Wang ML, Hu XQ, Beratan DN, Yang WT. Designing molecules by optimizing potentials. Journal of the American Chemical Society. 2006;**128**:3228-3232. DOI: 10.1021/ja0572046

[65] Lesiuk M, Balawender R, Zachara J. Higher order alchemical derivatives from coupled perturbed self-consistent field theory. The Journal of Chemical Physics. 2012;**136**:034104. DOI: 10.1063/1.3674163

[66] Bonaccorsi R, Scrocco E, Tomasi J. Molecular SCF calculations for the ground state of some three-membered ring molecules: $(CH_2)_3$, $(CH_2)_2NH$, $(CH_2)_2NH_2^+$, $(CH_2)_2O$, $(CH_2)_2S$, $(CH)_2CH_2$, and N_2CH_2. The Journal of Chemical Physics. 1970;**52**:5270-5284. DOI: 10.1063/1.1672775

[67] Campbell PG, Marwitz AJV, Liu S-Y. Recent advances in azaborine chemistry. Angewandte Chemie, International Edition. 2012;**51**:6074-6092. DOI: 10.1002/anie.201200063

[68] Kan M, Li Y, Sun Q. Recent advances in hybrid graphene-BN planar structures. Wiley Interdisciplinary Reviews: Computational Molecular Science. 2016;**6**:65-82. DOI: 10.1002/wcms.1237

[69] Kar T, Pattanayak J, Scheiner S. Rules for BN-substitution in BCN−fullerenes. Separation of BN and C domains. The Journal of Physical Chemistry. A. 2003;**107**:8630-8637. DOI: 10.1021/jp035744o

[70] March NH, Parr RG. Chemical potential, Teller's theorem, and the scaling of atomic and molecular energies. Proceedings of the National Academy of Sciences. 1980;**77**:6285-6288. DOI: 10.1073/pnas.77.11.6285

[71] Stuyver T, Fias S, De Proft F, Fowler PW, Geerlings P. Conduction of molecular electronic devices: Qualitative insights through atom-atom polarizabilities. The Journal of Chemical Physics. 2015;**142**:094103. DOI: 10.1063/1.4913415

[72] Aviram A, Ratner MA. Molecular rectifiers. Chemical Physics Letters. 1974;**29**:277-283. DOI: 10.1016/0009-2614(74)85031-1

[73] Sun L, Diaz-Fernandez YA, Gschneidtner TA, Westerlund F, Lara-Avila S, Moth-Poulsen K. Single-molecule electronics: From chemical design to functional devices. Chemical Society Reviews. 2014;**43**:7378-7411. DOI: 10.1039/C4CS00143E

[74] Goyer F, Ernzerhof M, Zhuang M. Source and sink potentials for the description of open systems with a stationary current passing through. The Journal of Chemical Physics. 2007;**126**:144104. DOI: 10.1063/1.2715932

[75] Ernzerhof M. A simple model of molecular electronic devices and its analytical solution. The Journal of Chemical Physics. 2007;**127**:204709. DOI: 10.1063/1.2804867

[76] Pickup BT, Fowler PW. An analytical model for steady-state currents in conjugated systems. Chemical Physics Letters. 2008;**459**:198-202. DOI: 10.1016/j.cplett.2008.05.062

[77] Stuyver T, Fias S, De Proft F, Geerlings P. Back of the envelope selection rule for molecular transmission: A curly arrow approach. Journal of Physical Chemistry C. 2015;**119**:26390-26400. DOI: 10.1021/acs.jpcc.51310395

[78] Solomon GC, Andrews DQ, Van Duyne RP, Ratner MA. When things are not as they seem: Quantum interference turns molecular electron transfer "rules" upside down. Journal of the American Chemical Society. 2008;**130**:7788-7789. DOI: 10.1021/ja801379b